PERGAMON

Journal of Structural Geology 23 (2001) 1659–1675

JOURNAL OF STRUCTURAL GEOLOGY

www.elsevier.com/locate/jstrugeo

Diagenesis-dependence of cataclastic thrust fault zone sealing in sandstones. Example from the Bolivian Sub-Andean Zone

Pierre Labaume[a,*], Isabelle Moretti[b]

[a]*Laboratoire de Géophysique Interne et Tectonophysique, BP 53, 38041 Grenoble Cedex 9, France*
[b]*Institut Français du Pétrole, 1–4 Avenue de Bois-Préau, 92852 Rueil-Malmaison, France*

Received 19 April 2000; revised 16 January 2001; accepted 23 January 2001

Abstract

Microstructural analysis of deformed sandstones in thrust fault zones of the Bolivian Sub-Andean Zone (SAZ) indicates that the porosity of fractures and cataclasites is primarily related to the occurrence or absence of quartz sealing resulting from local pressure solution and diffusive silica transport during deformation. Temperature was most probably the main factor that controlled quartz sealing and therefore the distribution of quartz sealing must be a function of the depth of burial at the time of deformation. Consequently, fault zones were sealed at depths exceeding about 3 km ($T > 70$–90°C), whereas shallower faults remain unsealed. In the SAZ, due to foothill uplift during fault activity, erosion reduced burial and allowed non-quartz-sealed fracturing to post-date quartz-sealed fracturing in critically buried fault segments. Most of the non-quartz-sealed faults were permeable to longitudinal carbonate-rich fluid flow. This distribution of quartz sealing is compatible with the current role of faults in oil migration in the SAZ and the foredeep. Therefore, we emphasise that the diagenetic conditions of deformation can play a major role in the variability of fault zone permeability in sandstones, this effect being independent of the fault type (normal or reverse) or fault offset. © 2001 Elsevier Science Ltd. All rights reserved.

Keywords: Fault zone; Sandstones; Quartz sealing

1. Introduction

The role of faults as drains or barriers is an important parameter of large-scale fluid flow in the upper crust, with major implications on fault dynamics and distribution of fluids, in particular hydrocarbons. In the oil industry, the sealing capacity of faults is commonly assessed by comparison of the porosity/permeability of rocks juxtaposed along the fault plane (e.g. Knipe, 1997), but the role of the specific petrophysical properties that fault rocks may acquire during and after deformation is less often taken into consideration. Nevertheless, these properties are important for assessing the role of faults in fluid flow. In particular, they can be used to determine specific hydraulic characteristics (permeability, thickness) attributed to fault zones as input parameters in a new generation of fluid flow numerical models (Moretti, 1998; Schneider et al., 1999).

In the case of siliciclastic sediments, studies of fault rock properties have mainly focused on mechanical processes at the origin of sealing, in particular clay smearing (e.g. Yielding et al., 1997) and sandstone cataclasis. In the latter case, microstructural and petrophysical investigations showed that grain-size reduction and compaction drastically reduce the porosity and permeability of faulted sandstones, making cataclasites potential seals for transversal fluid flow (Antonellini and Aydin, 1994; Fowles and Burley, 1994). In contrast, chemical processes, i.e. the sealing effect of diagenetic reactions that may be favoured by deformation, have been much less investigated (Sverdrup and Bjørlykke, 1992; Fisher and Knipe, 1998; Fisher et al., 2000).

In this paper, we describe deformation-related features developed in sandstones in thrust fault zones of the Sub-Andean Zone (SAZ) of southern Bolivia. The SAZ thrust faults affect a Palaeozoic to Tertiary siliciclastic succession about 10 km thick, thus providing a unique opportunity to investigate faulting processes in sandstones of different initial porosities and deformed in different burial (i.e. pressure–temperature) conditions. Based on the detailed study of microstructures and cement distribution in fault zones, we show that, in spite of different fracturing mechanisms dependent on sandstone initial porosity, the main sealing process is the precipitation of authigenic quartz in fractures and cataclasites. We discuss the possibility that the primary control of this sealing process was the temperature, i.e. the

* Corresponding author. Fax: +33-0476828101.
E-mail addresses: pierre.labaume@obs.ujf-grenoble.fr (P. Labaume), isabelle.moretti@ifp.fr (I. Moretti).

0191-8141/01/$ - see front matter © 2001 Elsevier Science Ltd. All rights reserved.
PII: S0191-8141(01)00024-4

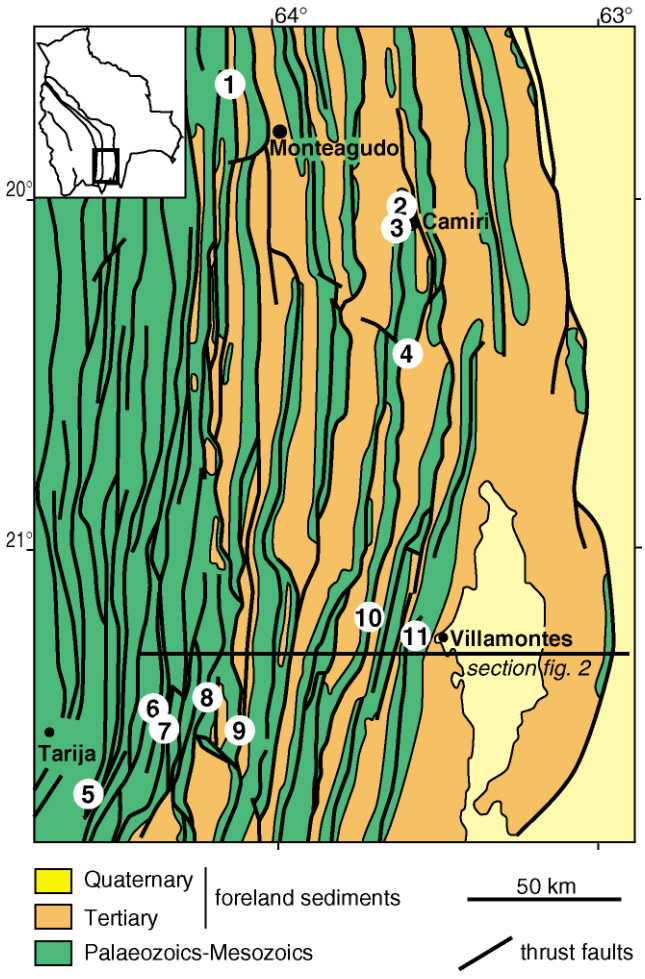

Fig. 1. Structural sketch of the study area. Numbers: location of the studied fault zones (1: Rio Azero; 2: upper Camiri; 3: lower Camiri; 4: Cuevo; 5: Tunal; 6: Piedra Larga; 7: Canaletas; 8: Honduras well; 9: Pajonal; 10: Rio Pilcomayo; 11: Aguarague). Inset: outline of Bolivia with Andean belt main thrusts and location of the study area (frame).

depth at which deformation occurred. This conclusion is consistent with the current fluid flow revealed by the distribution of oil seeps.

2. Geological setting

The SAZ is a Neogene foreland fold and thrust belt which constitutes the eastern border of the Andes. In the external SAZ of southern Bolivia (Fig. 1), the deformation is relatively recent and occurred mainly between 6 My and the present day (Gubbels et al., 1993; Moretti et al., 1996).

The stratigraphy of the southern Bolivian SAZ comprises a thick Cambrian to Quaternary succession above a Precambrian basement (Sempere, 1995). The thrust system involves the Upper Silurian to Quaternary succession, which is about 10 km thick. The Palaeozoic and Mesozoic series were deposited on a mainly siliciclastic platform. The lower series are marine, with about 4 km of Silurian and Devonian sand/shale alternations and 2 km of Carboniferous sandstones. Above occur a few hundreds of metres of Lower Permian fluvialeolian sandstones, a few tens of metres of evaporitic Upper Permian carbonates and Lower Triassic anhydrite/gypsum, and about 1 km of Upper Triassic to Cretaceous fluvial and eolian sandstones. The Upper Cretaceous and Paleogene are reduced to paleosoils overlain by the mainly fluvial Miocene to Recent foreland deposits. Paleo-thermometry analyses on outcrop and well samples show that the foreland succession commonly reached up to 3 km thick in the current foothills, but it was thinner (a few hundred metres) on the early anticlines (Moretti et al., 1996). The current foreland basin is around 3.5 km deep in the studied area.

The SAZ thrust system has an eastern vergence, with a main décollement level in the Silurian shales (Baby et al., 1993; Colletta et al., 1999) (Fig. 2). The average distance

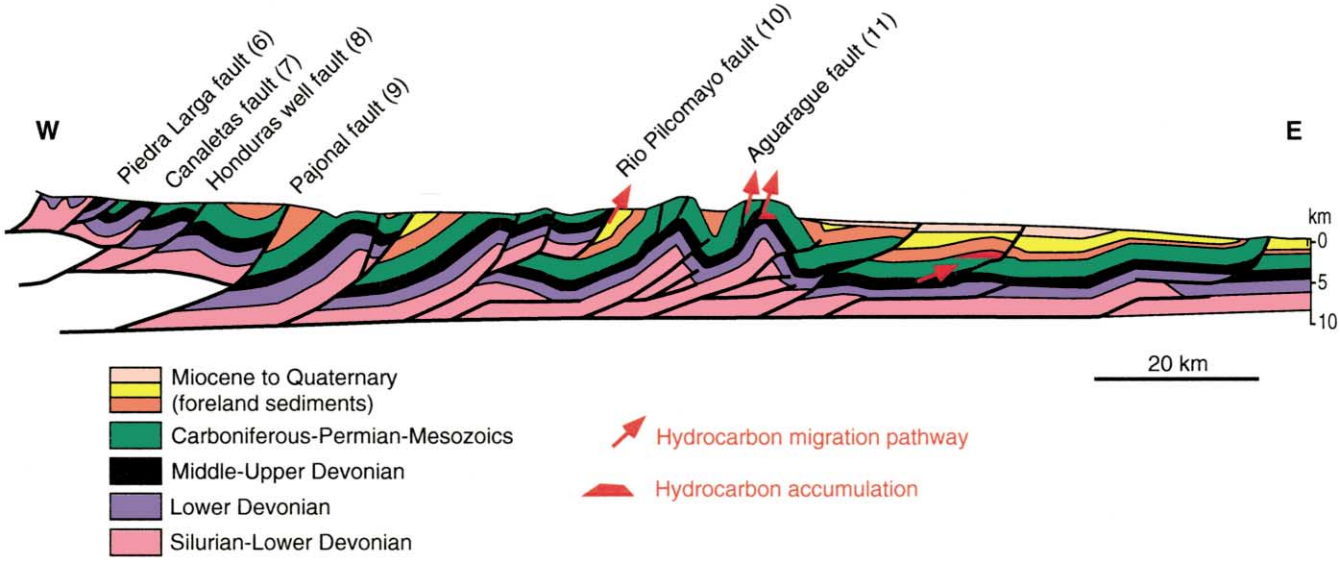

Fig. 2. Cross-section of the study area (location in Fig. 1; modified from Moretti et al. (1996); Colletta et al. (1999)). This section shows six of the studied fault zones (numbers after fault names correspond to those appearing in Fig. 1).

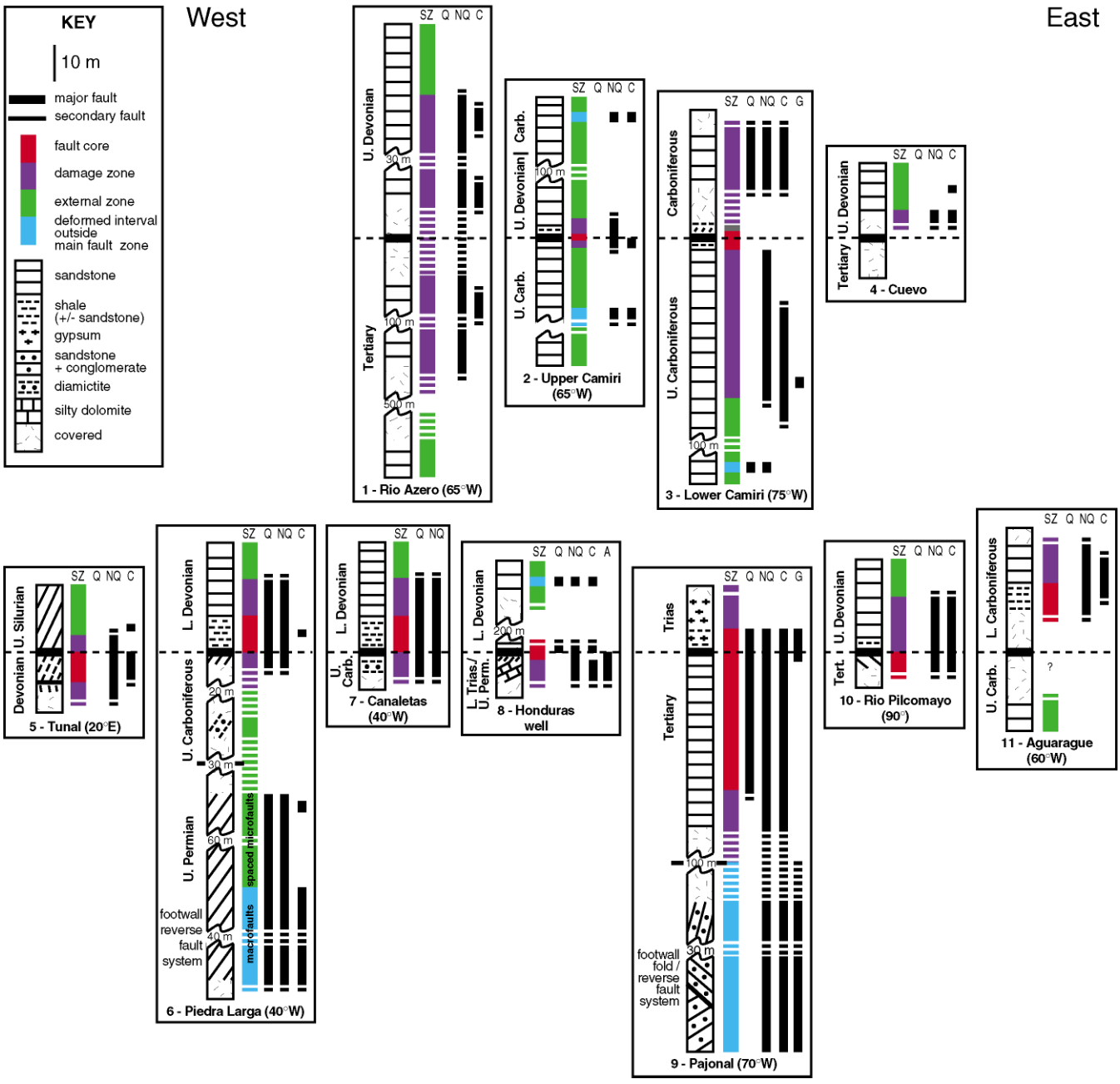

Fig. 3. Summary of the studied fault zones. The columns are set according to the relative location of the faults along two sections of the study area (cf. Fig. 1). For each fault, the column corresponds to the sampled section and shows the stratigraphic superposition, the lithologies involved, the fault zone structural zonation and the cement distribution. SZ: structural zonation; Q: quartz-sealed fractures and cataclastic slip bands (CSBs); NQ: non-quartz-sealed fractures and CSBs; C: carbonate (calcite or dolomite) cements in fractures, CSBs and/or host-sandstone; A, G: anhydrite and gypsum cements, respectively (post-carbonate cements). Spaced fractures and CSBs (Q and NQ) present in the external zones are not represented. On the other hand, the actual occurrence or absence of carbonate, anhydrate and gypsum cements is represented both inside and outside fault zones. For drawing simplification purpose, all faults are represented horizontally but the actual fault-bed angular relationships are shown to differentiate fault flats and ramps and the fault dips are indicated after the fault names.

between the thrust ramps is around 15 km and the displacement along individual thrusts is of several kilometers, up to 20 km. Some minor reverse faults affect the hinge of the thrust ramp anticlines and are related to secondary detachment levels in the Middle Devonian or Carboniferous shaly intervals. In the inner part of the SAZ, the basement is involved in the deformation (Kley et al., 1996).

3. Current fluid flow

The SAZ faults show different hydraulic behaviours with respect to the current hydrocarbon migration, in particular when comparing the foreland and the foothills. In the foreland, reverse faults act as seals in various hydrocarbon fields. In contrast, in the foothills, the classification of oil

seeps in relation to their structural position emphasises the capacity of faults and fractures to focus oil migration: 60% of the oil seeps leak from large thrust faults, 30% from the hinge of the anticlines and only 10% from monoclines (Labaume and Moretti, 1997).

4. Studied faults

We studied 11 faults distributed along two sections across the whole SAZ (Fig. 1). Seven faults are large thrusts (Rio Azero, Cuevo, Piedra Larga, Canaletas, Honduras, Pajonal, Rio Pilcomayo), one is a back-thrust (Tunal) and three are minor (a few hundred metres offset) reverse faults in thrust ramp anticlines (upper and lower Camiri, Aguarague). All faults were studied in outcrops, except the Honduras fault which was studied on well cores recovered at about 2450 m depth. The different stratigraphic superpositions observed across the fault planes are: Palaeozoic above Palaeozoic (upper and lower Camiri, Tunal, Piedra Larga, Canaletas, Aguarague), Palaeozoic above Triassic (Honduras), Palaeozoic above Tertiary (Rio Azero, Cuevo, Rio Pilcomayo) and Triassic above Tertiary (Pajonal) (Fig. 3). Structural restorations constrained by paleo-thermometry analyses (Moretti et al., 1996) show that, in the case of the large thrusts, the burial of the various studied fault-rocks at the beginning of deformation was between a few hundred metres (Tertiary) and up to about 7–8 km (Lower Devonian at Piedra Larga and Canaletas). The depth at the beginning of deformation is less well constrained in the case of the reverse faults in anticlines, because they are late structures that may have begun to form after substantial erosion of anticline crests. Paleo-thermometry analyses on well samples from the Camiri oil field show that the anticline to which the two Camiri faults belong was buried under less than 1500 m of Tertiary (Moretti et al., 1996), which implies that the Upper Carboniferous samples from these outcrops were buried no more than 3 km deep. Pre-thrust erosion is also possible in the case of the Tunal back-thrust.

5. Method of study

For each fault, the "fault zone" was qualitatively defined as the interval around the fault surface displaying a higher concentration of deformation-related features (fractures, minor faults, folds, mineral veins, etc.) than is typically present in the host-rocks far from the fault (Chester and Logan, 1986). A structural analysis was carried out along a profile transverse to the fault zone in order to identify the types and distribution of these fault-related deformation structures. The length of the profile was determined such as to cover the whole fault zone and a few tens to hundreds of meters of the adjacent host-rocks, except in the cases where observation was limited by the lack of outcrop (Fig. 3). Representative samples of the deformation-related features were collected in the fault zone, as well as samples of the adjacent country rocks. A few samples of most of the stratigraphic formations were also collected far (up to several km) from the fault zones, in order to better assess background diagenesis, deformation and fluid flow.

Approximately 250 thin sections of colored epoxy resin-impregnated samples were examined using petrographic and scanning electron microscopes (SEM) for petrographic and microstructural study. The SEM was coupled with an energy dispersive system (EDS) for qualitative and semi-quantitative element analyses. Cathodoluminescence (CL) of carbonates was studied with a cold-cathode system on a petrographic microscope and CL of quartz was studied with a SEM. Porosity was estimated by image analysis under the petrographic microscope and was measured by the mercury injection technique on a few samples. Kaolin polytypes were analysed by X-ray diffraction.

6. Fault zone macrostructure

The fault-bed angular relationships define either fault flats or ramps (Fig. 3). Several faults feature a hanging wall flat with a few decimetre- to metre-thick basal detachment horizon comprising alternations of shale and sandstone beds (upper and lower Camiri, Piedra Larga, Canaletas, Rio Pilcomayo, Aguarague) or shale and gypsum beds (Pajonal).

The fault zones are a few metres to hundreds of metres thick and their internal structure can be described using the damage zone-fault core model (Chester and Logan, 1986; Caine et al., 1996) (Fig. 3). The fault core is defined as the interval where a high concentration of deformation resulted in a strong bedding disturbance and the damage zones as the peripheral intervals with weaker deformation and globally preserved bedding. The frequency of fracture connection is higher in the fault core than in the damage zones. In some cases, intervals affected by weak fault-related deformation occur outside (up to a few ten to hundred meters) from the main fault zone (upper and lower Camiri, Piedra Larga, Pajonal; Fig. 3). For simplification purpose in the following text, the term 'fault zone' is used for both the main fault zone and these peripheral deformed intervals.

The most frequent lithology involved in fault zones are sandstones. The main deformation structures in sandstones are cataclastic slip bands (Fig. 4A) and shear and extension fractures (Fig. 4B). Depending on the case, these structures may or may not be cemented by quartz, carbonate or gypsum. Where a shale-rich layer forms a hanging wall detachment horizon, it concentrated the deformation and represents the fault core, with a sheared shale matrix and truncated sandstone beds (gypsum beds at Pajonal) (Fig. 4B).

The kinematics of structures in fault zones is complex in detail and varies from one fault to the other. However, deformation in hanging wall detachment horizons mainly

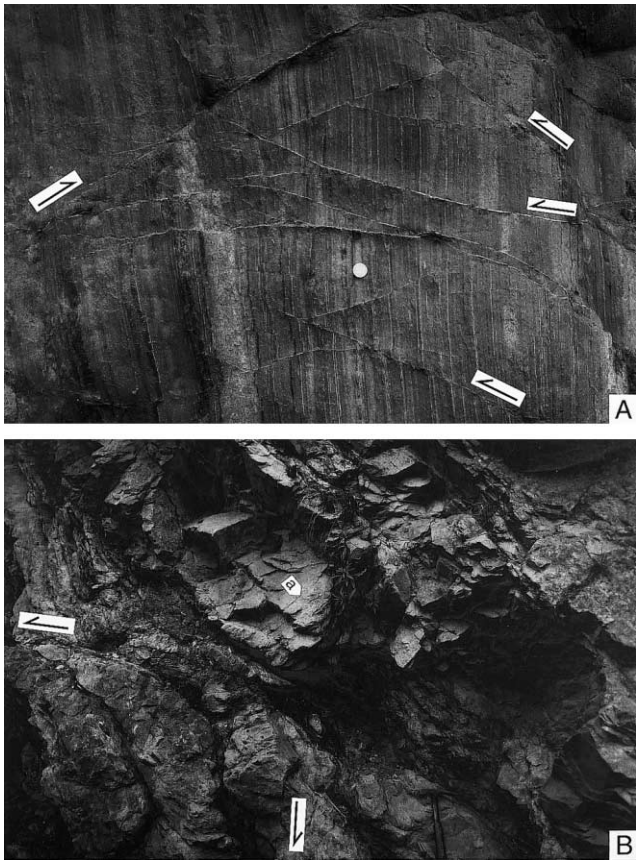

Fig. 4. Aspect of fault zones in sandstones. (A) Set of cataclastic slip bands with centimetre-offsets (arrows) corresponding to reverse faults in vertically bedded porous sandstones (Lower Permian, Piedra Larga fault, footwall reverse fault system). (B) Shear (arrows) and extension (a) fractures corresponding to bedding-parallel extension in low-porosity sandstones. Beds dip to the right (Lower Devonian, Canaletas fault, hanging wall fault core).

corresponds to bedding-parallel extension (Fig. 4B), whereas deformation in footwall ramps is dominated by sub-horizontal compression (Fig. 4A).

7. Sandstone petrology and sedimentary burial compaction

In all of the studied formations, the sandstone composition is of 70–80% quartz grains and 10–20% alkali feldspar grains. Other grains (0–10%) are mainly micas, clays and rock fragments. There are no early cements except local quartz cements with chalcedony to macrocrystalline texture in Lower Permian sandstones.

The degree of sandstone compaction related to sedimentary burial is assessed by the study of samples collected outside the fault zones, in order to avoid possible compactional effects of faulting deformation. Porosity of unfaulted sandstones is high (up to about 20% estimated by image analysis) in the upper part of the succession, where compaction is mainly mechanical and chemical compaction is absent or very little developed (Fig. 5A). Chemical compaction affects quartz and feldspar grains and is characterised by the combination of intergranular pressure solution and precipitation of overgrowths (e.g. Houseknecht, 1988) (Fig. 5B and C), and is interpreted to result from the temperature increase with depth (see discussion below, Section 9). In the SAZ, the development of chemical compaction in unfaulted sandstones becomes high between the Mesozoic and Upper Carboniferous formations. The structural distribution of the upper boundary of chemical compaction shows that it occurs at stratigraphic levels that experienced a maximal sedimentary burial of about 3 km, this level varying with the local thickness of the Tertiary. Hence, chemical compaction is well developed in the Triassic samples from the hanging wall of the Pajonal fault, whereas it is lacking or incipient in the Upper Carboniferous samples from the Camiri area where the thickness of the Tertiary was reduced (see above, Section 4). The intensity of chemical compaction increases downward and results in a strong reduction of porosity. Consequently, all the samples below the Upper Carboniferous show little preserved intergranular porosity under the petrographic microscope (Fig. 5B and C). Porosities of less than 5% were measured by the mercury injection technique in Lower Devonian samples from the Honduras well (Huamampampa Formation) and Piedra Larga outcrop (Santa Rosa Formation). That chemical compaction begins to develop around 3 km depth and strongly contributes to porosity reduction below this depth is concordant with observations in other siliciclastic basins (e.g. Bjørlykke and Egeberg, 1993).

Sandstone diagenesis during sedimentary burial is also marked by the partial dissolution of feldspar grains and by the precipitation of kaolin, both features being relatively common in unfaulted sandstones of all formations. X-ray analyses performed on a few samples show that kaolin is mainly kaolinite with local small amounts of dickite in the Upper Carboniferous sandstones of the Camiri area and dickite in Upper Devonian sandstones at Rio Pilcomayo and Lower Devonian sandstones at Piedra Larga. As explained above, the maximum burial of the Upper Carboniferous sandstones of Camiri was no more than 3 km, whereas that of the Devonian sandstones was of at least 5 km. Similarly to observations made in other basins, feldspar dissolution and kaolinite precipitation probably represent rather shallow diagenesis related to the circulation of meteoric water (Bjørlykke, 1994) and the depth distribution of kaolin polytypes results from the temperature-dependent kaolinite to dickite transformation during burial (Ehrenberg et al., 1994).

8. Fault zone microstructures in sandstones

Deformation of sandstones in the SAZ fault zones is dominated by brittle processes that may be associated, or

not, with pressure solution and sealing by authigenic quartz. In both cases, the characteristics of fracturing are closely related to the pre-faulting porosity of the host-sandstone. Below, we first describe the microstructures without quartz sealing, then those with quartz sealing.

8.1. Microstructures without quartz sealing

8.1.1. Porous sandstones

In porous sandstones, fractures are mostly intragranular: individual fractures generally do not pass from one grain to the other and their geometry shows that they were generated by stress concentration at grain contacts (Fig. 6A). Most fractures are extensional but they show variable patterns, from domains with a low density of sub-parallel fractures to completely crushed grains. The localisation of deformation resulted in the formation of millimetre-thick shear zones characterised by strong grain size reduction (Figs. 4A and 6B–D).

In most cases, the cataclastic shear zones are similar to those described in other examples of faulted porous sandstones (e.g. Aydin and Johnson, 1983; Antonellini et al., 1994; Fowles and Burley, 1994). According to the terminology of Fowles and Burley (1994), we refer to these shear zones as cataclastic slip bands (CSBs). The observation of CSBs at various stages of evolution show that their formation initiated by the concentration of intragranular fractures that are arranged en-échelon. With increasing shear displacement, the microlithons separated by the fractures rotated, which resulted in the formation of new fractures and opening of fracture porosity (Fig. 6B). Eventually, the grain fragments collapsed, resulting in the typical microstructure of ‘mature’ CSBs, characterised by a strongly reduced porosity compared with that of the host-sandstone (Fig. 6C and D) (see also Antonellini and Aydin, 1994; Fowles and Burley, 1994). Where mica grains and/or clay and oxide accumulations are present, they were smeared along the CSBs (Fig. 6C and D). The intensity of grain fracturing inside CSBs is usually very heterogeneous, with coexisting intact and more or less intensely crushed grains, resulting in the lack of clear organisation of the fracture pattern. This observation emphasises the mechanical heterogeneity of porous sandstones, where deformation concentrates in the most stressed grains, thus protecting the other grains from fracturing. However, a transverse gradient of deformation is observed in some CSBs, with a central zone where the localisation of shear movement induced

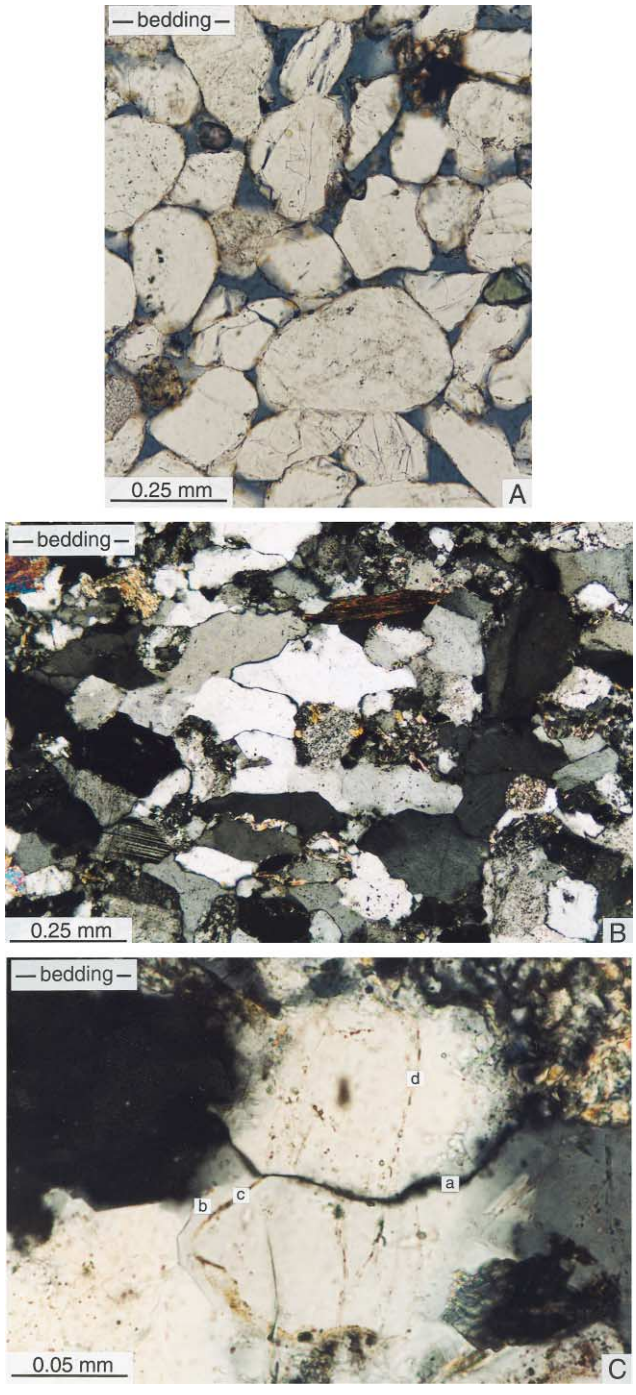

Fig. 5. Sandstone microtextures resulting from sedimentary burial compaction in samples collected outside fault zones. (A) Porous sandstone typical of the upper part of the stratigraphic succession (Tertiary). Maximal sedimentary burial is estimated at no more than 1000 m. The sandstone features high primary porosity (blue: impregnation epoxy resin in pores and fractures) and moderate compaction with pressure solution contacts and intragranular fractures. The latter microstructures may, at least in part, correspond to the tectonic deformation related to the Rio Azero thrust located about 500 m westward (Rio Azero fault footwall; plain light microphotograph). (B) Low-porosity sandstone typical of the lower part of the stratigraphic succession (Silurian Tarabucco Formation). Maximal sedimentary burial is estimated at about 8000 m. The sandstone features high grain imbrication and bedding-parallel shape fabric resulting from chemical compaction. No porosity is visible with the petrographic microscope (Tunal fault hanging wall; crossed polarisers microphotograph). (C) Detail of chemical compaction features in low-porosity sandstones. (a) Pressure solution at grain contact related to bedding-normal shortening; (b) quartz overgrowths; (c) original detrital grain boundary marked by iron oxide coating and fluid inclusions; (d) healed intragranular fractures (now marked by alignments of fluid inclusions) related to bedding-normal shortening (Middle Devonian Los Monos Formation, Aguarague anticline hinge zone; crossed polarisers microphotograph).

strong grain size and porosity reduction and peripheral zones with weaker fracturing and open fracture porosity. The host-sandstone can be affected by more or less abundant distributed intragranular fractures (Fig. 6C).

In most cases, the offset and thickness of CSBs do not exceed a few millimetres and cohesion was not lost across the CSB. With larger displacement, a through-going discrete fracture may have formed inside or at the border of the CBS and concentrated displacement. At outcrop, these surfaces bear thin striations parallel to slip direction.

Some CSBs differ from the common microstructure described above by the occurrence of a well-developed S–C fabric geometrically analogous to that of metamorphic fault rocks (Berthé et al., 1979; Lister and Snoke, 1984) (Fig. 6E and F). However, contrary to the metamorphic rocks where deformation is dominated by plastic shearing and dynamic recrystallisation, the S–C microstructures described here result from a cataclastic process. The major shear displacement is materialised by thin bands of intensely crushed grains and smeared clay and oxide accumulations (C-surfaces). Between them is developed a rough oblique S-foliation with a sigmoidal geometry, underlined by clay and oxide seams. CL–SEM images allow for the differentiation of the different detrital grains and show that the foliation results from the cataclastic flattening of detrital grains, achieved by an often extremely strong grain comminution and rearrangement of grain fragments. SEM images also show the lack of pressure solution at grain fragment contacts and of authigenic quartz precipitation in fractures (Fig. 6G). The less deformed grains can be affected by a few through-going intragranular shear or extension fractures (Fig. 6E and F). The C-surfaces, sigmoidal S-foliation and through-going intragranular fractures are all compatible with a shortening direction sub-perpendicular to the S-foliation. This allows the through-going intragranular fractures to be defined in the terms of the Riedel system (e.g. Logan et al., 1992), with T extension fractures sub-perpendicular to the foliation, and R and X shear fractures synthetic and antithetic to the general shearing, respectively (Fig. 6E and F).

To our knowledge, such foliated cataclastic microstructure has not previously been described in naturally deformed sandstones, but it was recently observed in porous sandstones deformed by laboratory triaxial compression (Mair et al., 2000). In contrast, foliated cataclasites are common in other types of quartz-bearing rocks such as granite or schist, where their development is interpreted as being due to the presence of feldspar and/or clays/micas (e.g. Chester et al., 1985; Evans, 1988; Schulz and Evans, 1998; Lin, 1999). In this interpretation, the weaker grains (feldspar and phyllites) are preferentially fractured, rotated and altered, resulting in the formation of a matrix affected by ductile flow at the aggregate scale, whereas the less deformed quartz grains are isolated in the matrix (Mitra, 1984). In the microstructures described here, the role of mineralogical composition is not clear, as the CSBs with and without foliation all formed in sandstones with similar feldspar and clay content, and extreme grain crushing similarly affects quartz and feldspar grains in the foliated CSBs. In fact, we observe that foliation only developed in CSBs typically thicker than about 1 cm and featuring through-going striated slip surfaces. This suggests that a sufficient thickness of the CSB compared with the grain size, combined with a sufficient shear displacement, were necessary conditions to allow for the geometrical rearrangement of grain fragments producing the foliation.

8.1.2. Low-porosity sandstones

In low-porosity sandstones, the higher mechanical homogeneity compared with porous sandstones (i.e. the lower mechanical influence of grain contacts) favoured the formation of transgranular fractures that can cross several grains and reach up to several decimetres long (Fig. 7A). They are shear or extension fractures that can be grouped into millimetre-thick shear zones organised as Riedel systems (Fig. 7B). Development of shear zones locally resulted in a high density of fractures giving a microstructure analogous to that of the CSBs in porous sandstones.

8.1.3. Depth-distribution of the different fracturing types

The typical intragranular fracturing is found in the upper part of the section, from the Tertiary to the Upper Carboniferous formations where porosity is higher than 10%, generally around 20%. The typical transgranular fracturing occurs in the lowermost part of the section (Silurian, Devonian) where porosity is lower than 5%. In the intermediate part of the section, i.e. mainly from the Lower Permian to the Upper Devonian, sandstones with intermediate porosity exist, which show an intermediate fracturing process due to the weak cohesion of grain contacts. In this case, fractures are mostly transgranular but they often have a sinuous geometry because they contain many segments that follow grain contacts rather than cutting the grains, and sets of closely-spaced fractures may have evolved into CSBs.

8.1.4. Carbonate or gypsum cementation

The non-quartz-sealed microstructures can show a fracture porosity that remained empty (Figs. 6 and 7), or they can be cemented by carbonate (generally calcite, locally dolomite; Figs. 7B and 8), locally by gypsum. Carbonate cementation is common and is observed in 10 of the 11 studied fault zones (Fig. 3). Gypsum cement is rare and occurs in a significant amount only in the Pajonal fault zone (Fig. 3). In the CSBs, the precipitation of carbonate usually implied a strong dilation of the cataclastic texture, with detrital grain fragments floating in the cement (Fig. 8A). Carbonate or gypsum precipitation in transgranular fractures resulted in the formation of veins up to a few millimetres-thick with carbonate (Fig. 8B) and a few centimetres-thick with gypsum. Usually, the same cement

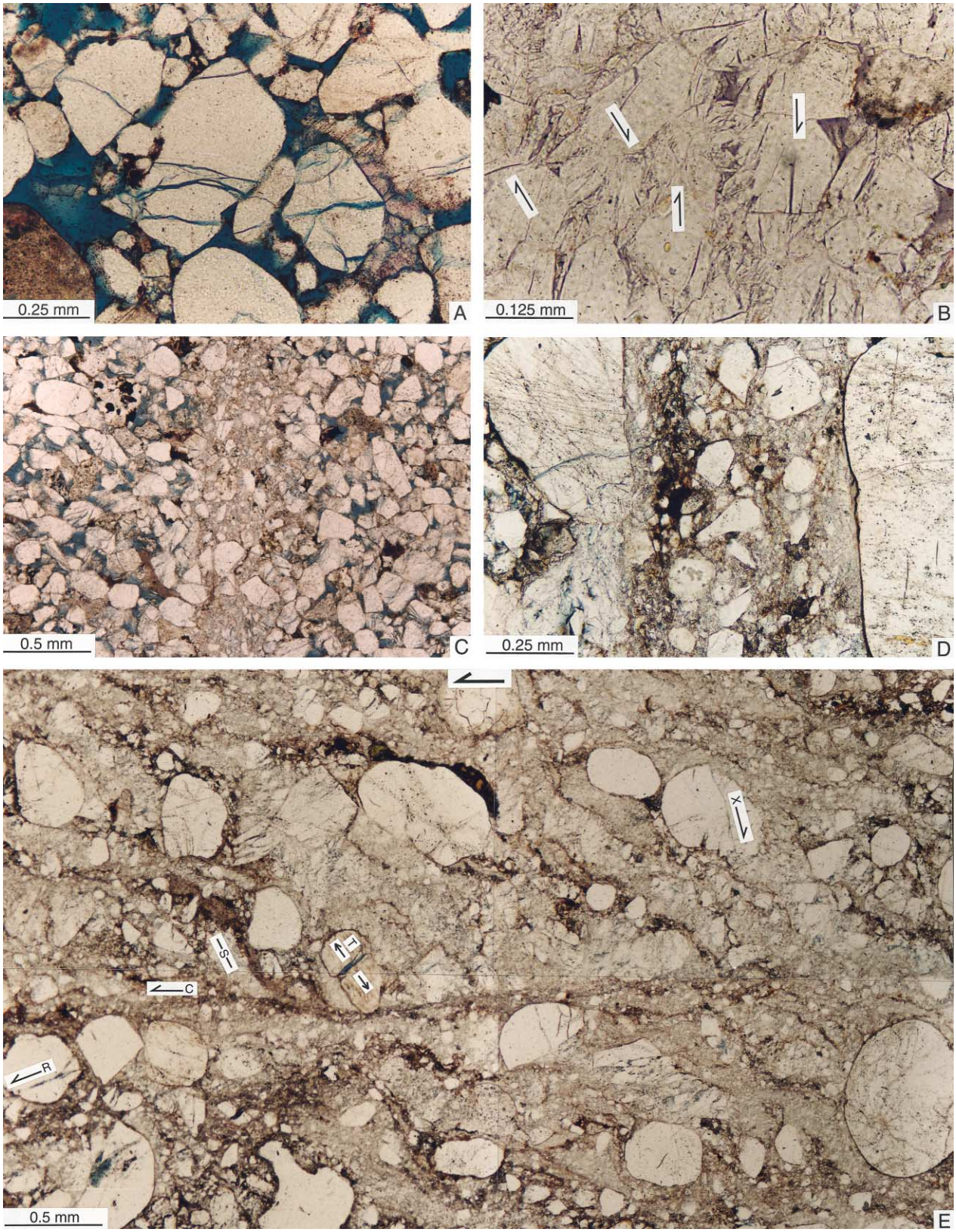
0.25 mm
A
0.125 mm
B
0.5 mm
C
0.25 mm
D
X
S
C
R
0.5 mm
E

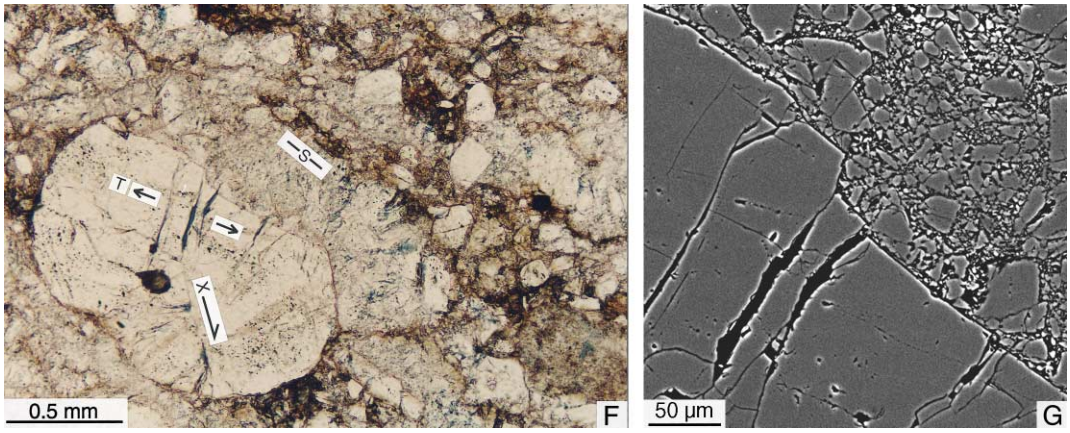

Fig. 6. (*continued*)

that precipitated in the CSBs or veins is also present in their host-sandstone, the mineralogical, textural and CL characteristics arguing for coeval precipitation. Cementation is rarely complete at the centimetre-scale, i.e. part of the fracture and matrix porosity is generally preserved (Figs. 7B and 8B). In the carbonate veins, this resulted in the formation of geodic structures (Fig. 8B).

8.2. Microstructures with quartz sealing

Quartz-sealed microstructures are CSBs in porous sandstones and transgranular fractures in low-porosity sandstones, the general characteristics of which are similar to those of the microstructures described above, but they differ by the occurrence of authigenic quartz cement. Another characteristic is that they commonly comprise pressure solution features affecting the quartz and feldspar grains.

8.2.1. Porous sandstones

In the CSBs, the authigenic quartz is difficult to differentiate under the optical microscope because it forms domains that are very small (micron-scale) and intricately associated with the detrital grain fragments. However, the quartz-sealed CSBs can be differentiated from the non-quartz sealed CSBs by their highly sutured grain fragments when observed under crossed polarisers and by their non-porous texture with quasi non-differentiable grain fragments when observed in plain light (Fig. 9A and B, to compare with Fig. 6C and D). Under the optical microscope, another difference with the non-quartz-sealed CSBs is the rareness of visible fractures in grains at the CSB periphery. The intimate microstructure of the quartz-sealed CSBs is better appreciated on CL–SEM images. This technique allows for the differentiation of detrital and authigenic quartz (Milliken, 1994; Dickinson and Milliken, 1995) and shows that quartz-sealing of CSBs implied dilation of the cataclastic texture, with grain fragments floating in the cement (Fig. 9C and D). CL–SEM images also show that the density of quartz-sealed intragranular fracture is usually very high at the periphery of CSBs (Fig. 9E and F), although these fractures are hardly visible in optical microscopy. This discrepancy is due to the fact that the fractures are very thin (a few microns) and filled by quartz in crystallographic continuity with that of detrital quartz. Comparison of images obtained by both techniques also shows that the irregular extinction that is commonly observed in these fractured grains between crossed polarisers (Fig. 9B) is not due to crystal plastic deformation, but to the fact that the grain fragments rotated before the precipitation of authigenic quartz. The fractured grains at the CSB periphery often show indented grain contacts characterised by the association of pressure solution at grain contacts and quartz-sealed intragranular fractures originating at the same contacts (Fig. 9E and F).

Similarly to the non-quartz-sealed CSBs, the quartz-sealed cataclasites may show a S–C fabric. In this case, the cataclastic S-foliation is also marked by pressure

Fig. 6. Fault zone microstructures without quartz-sealing in porous sandstones (except (G), all images are plain light microphotographs; on these, blue is impregnation epoxy resin in pores). (A) Intragranular fractures related to stress concentration at grain contacts (Upper Carboniferous, upper Camiri fault zone). (B) Incipient cataclastic slip bands (CSBs, arrows), with en-échelon intragranular fractures at various stages of rotation and opening of fracture porosity (Upper Carboniferous, upper Camiri fault zone). (C) 'Mature' CSB. Note the strong grain size and porosity reduction in the band, and distributed intragranular fractures and preserved porosity in the host-sandstone (Tertiary, Cuevo fault zone). (D) Detail of cataclastic fabric in a CSB (Tertiary, Rio Azero fault zone). (E) Internal structure of a CSB featuring a well-developed S–C fabric. S: foliation; C: shear surface parallel to general shearing; R and X: shear fractures synthetic and antithetic of general shearing, respectively; T: extension fracture (Tertiary, Rio Azero fault zone). (F) Detail of the S–C fabric shown in (E) (letters as in (E)). (G) Detail of (F) (center left), on a back-scattered SEM image showing preserved porosity (in black) and the lack of pressure solution at grain fragment contacts. The cathodoluminescence-SEM image (not shown here) reveals the lack of authigenic quartz precipitation.

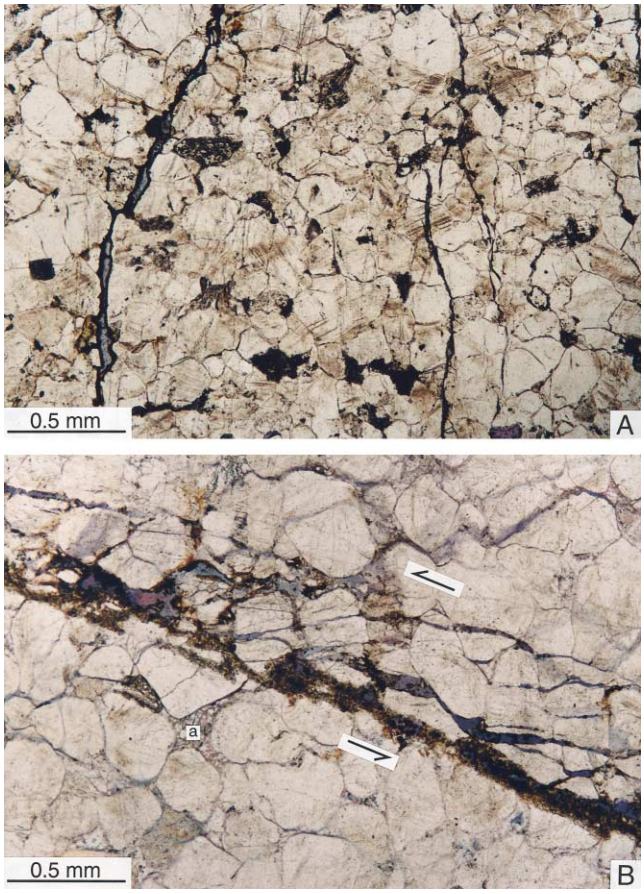

Fig. 7. Fault zone microstructures without quartz sealing in low-porosity sandstones (plain light microphotographs; blue: epoxy resin in pores). (A) Extensional transgranular fractures. The fractures are partially filled by iron oxide (dark material), probably formed recently close to the surface (Lower Devonian, Piedra Larga fault zone). (B) Set of intragranular and transgranular fractures forming a Riedel shear system (arrows). They are partially filled by calcite cement, covered by iron oxide (dark material), but some fracture porosity is preserved. (a) Calcite cement in host-sandstone coeval to that in fractures, as shown by CL observation (Lower Permian, Piedra Larga fault zone).

solution seams, preferentially developed along clay- and oxide-rich accumulations (Fig. 9G and H), and SEM images show microstylolites related to grain fragment indentation by pressure solution (Fig. 9I).

The almost complete quartz sealing and compaction resulting from pressure solution give these CSBs a very low porosity. However, the peripheral zones of CSBs usually show quartz cement only in the transgranular fractures and original intergranular porosity is preserved (Fig. 9C and E).

8.2.2. Low-porosity sandstones

In low-porosity sandstones, the transgranular fractures are sealed by quartz, thus forming veins up to a few millimetres thick (Fig. 9J). The veins are associated with pressure solution seams (stylolites) developed along mica-rich layers.

8.3. Occurrences and chronology of quartz-sealed and non-quartz-sealed microstructures

Six of the studied fault zones display only microstructures without quartz sealing (upper Camiri, Rio Azero, Cuevo, Tunal, Rio Pilcomayo, Aguarague) and five display both quartz-sealed and non-quartz-sealed microstructures (lower Camiri, Piedra Larga, Canaletas, Honduras, Pajonal) (Fig. 3).

Microstructures with quartz sealing have been observed in the Lower Devonian (Piedra Larga, Canaletas, Honduras), Lower Carboniferous (Piedra Larga, Canaletas), Upper Carboniferous (lower Camiri), Upper Permian (Piedra Larga) and Tertiary (Pajonal). Microstructures without quartz sealing are observed in all the formations involved in all the studied fault zones, from the Silurian to the Tertiary. In the cases where the two fault zone compartments are visible at outcrop, each type of microstructure (i.e. with or without quartz sealing) represented in the fault zone was observed in both compartments. Most of the quartz-sealed microstructures are CSBs. A few quartz-filled veins have been observed only in the hanging wall part of the Piedra Larga, Canaletas and Honduras well fault zones, i.e. in the sandstones that have the lowest porosity (<5%) among those featuring quartz-sealed microstructures (Lower Devonian).

Cross-cutting relationships show that the microstructures without quartz sealing systematically post-date those with quartz sealing (Fig. 10). When carbonate cement is present in the non-quartz-sealed microstructures, its precipitation is often associated with dissolution/replacement of quartz, thus resulting in the formation of irregularly-shaped carbonate patches across the older quartz-sealed cataclasite (Fig. 10B).

We have never observed the chronology opposite to that described above, or fault zones featuring only quartz-sealed microstructures.

9. Discussion

The descriptions above show that the deformation processes affecting sandstones in the SAZ fault zones were dependent on the diagenetic conditions from two aspects.

Firstly, the type of fracturing was controlled by the degree of diagenesis reached before faulting, with mostly intragranular fracturing in porous sandstones and transgranular fracturing in low-porosity sandstones. The correspondence between these fracturing types and the present host-sandstone porosity shows that fault zone deformation occurred after most of the burial compaction was achieved, i.e. that faults are recent structures formed when (most of) the Tertiary foreland sediments were already deposited. This conclusion is consistent with the kinematic analysis of large-scale structures (see above, Section 4).

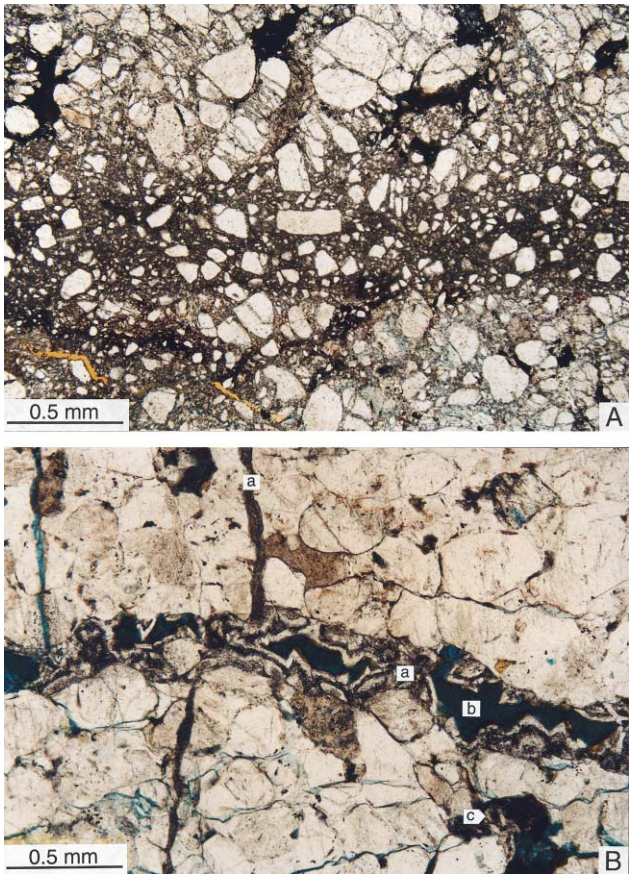

Fig. 8. Carbonate cementation in fault zone microstructures without quartz sealing (plain light microphotographs; blue: impregnation epoxy resin in pores). (A) Cataclastic slip band (CSB) with abundant dolomite cement (dark material). Cement precipitation implied dilation of the cataclastic fabric and separation of grain fragments that float in the cement. Dolomite is also abundant as intergranular and microfracture cement in the host-sandstone (Tertiary, Rio Pilcomayo fault zone). (B) Dolomite veins (a) in transgranular fractures in low-porosity sandstone; (b) geodic cavity partially filled with iron oxide, probably formed recently close to the surface; (c) zoned dolomite crystal coeval to the vein which precipitated in a secondary pore due to feldspar dissolution in the host-sandstone (Upper Devonian, Rio Pilcomayo fault zone).

Secondly, the conditions of diagenesis during faulting controlled the presence or absence of microstructure quartz-sealing. The discussion below concerns this aspect and its implications on the hydraulic behaviour of faults. In the samples observed, fluid inclusions in authigenic quartz cementing microstructures are scarce and smaller than 2 μm, which is close to the size limit of applicability of microthermometry techniques. Fluid inclusion study is also made difficult by the fact that detrital and authigenic quartz in cataclasites are intricately associated and virtually impossible to differentiate under the optical microscope. For these reasons, we lack the pressure-temperature data that fluid inclusion study may have provided for constraining the conditions of quartz sealing. Below, these conditions are discussed in the light of theoretical considerations and other natural examples of quartz sealing described in the literature and relevant to the textural and chronological features observed in the SAZ microstructures.

9.1. Origin of the authigenic quartz in fault zone microstructures

Quartz cementation is the final product of a three-step process: dissolution, transport and precipitation. The question of the origin of quartz covers the determination: (i) of the sites and processes of dissolution, which can occur on free or stressed surfaces and (ii) of the mechanism of transport that can be achieved by fluid flow (advection) or diffusion.

In the case studied here, the quartz-sealed microstructures systematically show the evidence of pressure solution features (indented grain contacts or stylolites) affecting quartz and feldspar grains, whereas these features are absent or very scarce in the non-quartz-sealed microstructures. The geometrical relationships show that pressure solution features are coherent with the centimetre-scale stress pattern responsible for local fracturing. Fig. 9E and F shows an indented grain contact where compression sub-normal to the contact explains both pressure solution at the contact and the fan geometry of the intragranular extensional fractures that initiate at the contact in both grains. Fig. 9G and H shows a pressure solution foliation compatible with other shear sense criteria in an S–C cataclastic fabric. Fig. 9J shows stylolitic seams and a quartz-filled vein, both compatible with bedding-normal compression. These observations suggest that fracturing and pressure solution were associated deformation mechanisms and that the quartz that precipitated in the fractures was, at least in part, derived from the neighbouring pressure solution microstructures and transported over a short distance by diffusion. In this interpretation, transfer of silica was driven by the gradient between the high, stress-enhanced, chemical potential at grain contacts, which promotes dissolution and the lower chemical potential on the free grain surfaces where precipitation occurs (e.g. Rutter, 1983; Green, 1984; Renard et al., 2000).

The assumption of a local origin of quartz is also coherent with geochemical modelling. Indeed, when transported by diffusion, most of the dissolved silica precipitates at small ($<$1 m) distances from the dissolution site (Bjørlykke and Egeberg, 1993; Oelkers et al., 1996). A more distant origin would have necessitated transport of the dissolved silica by fluid advection but this is an unlikely mechanism for complete cementation of fractures by quartz in the conditions of basin diagenesis, due to the unrealistically high amount of fluid required (Pedersen and Bjørlykke, 1994).

The formation of dense fracture networks in fault zones is likely to have favoured the efficiency of local transfer of silica:

- In the pressure solution model, fracturing partitions the grain contacts where dissolution occurs and thus

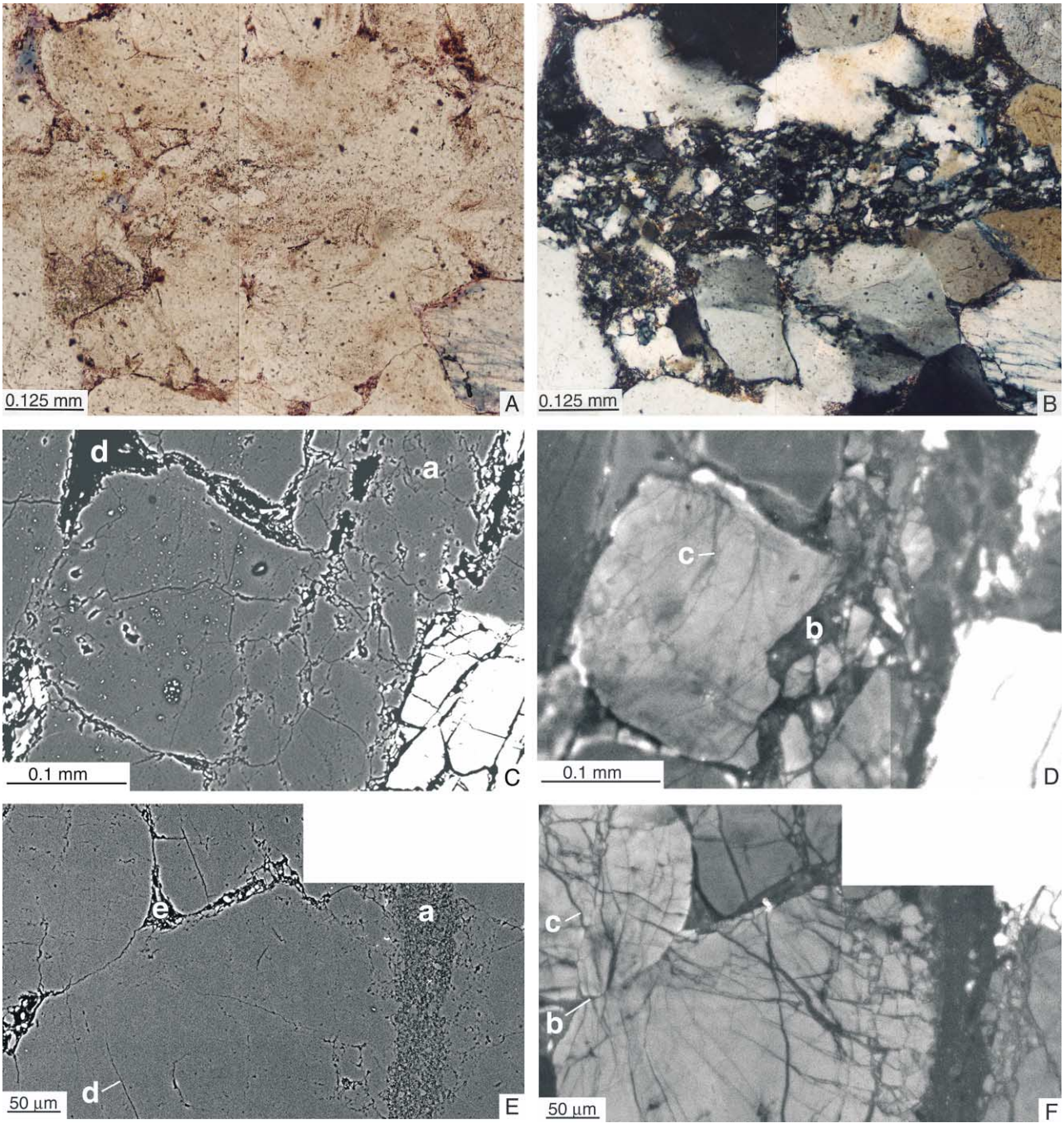

Fig. 9. Fault zone microstructures with quartz sealing. (A and B) Plain light (A) and crossed polarisers (B) microphotographs of a cataclastic slip band (CSB). In (B), note the strong indentation of grain fragments inside the CSB and irregular extinction in grains at the CSB periphery. These grains are also characterised by the scarcity of visible intragranular fractures. In (A), note the very low porosity (blue: epoxy impregnation resin in pores) and poorly differentiable grain fragments inside the CSB, to compare with unsealed cataclasite shown in Fig. 6C and D (Lower Permian, Piedra Larga fault zone). (C and D) Back-scattered (C) and cathodoluminescence (D) SEM-images of a CSB (a) and peripheral zone. In (C), dark grey is quartz, white is K-feldspar and black is porosity. In (D), authigenic quartz appears in black. It precipitated between grain fragments in the CSB (b) and thin intragranular fractures in the peripheral zone (c). Note the very low porosity in the CSB and preserved intergranular porosity in the peripheral zone (d) (Lower Carboniferous, Piedra Larga fault zone). (E and F) Back-scattered (E) and cathodoluminescence (F) SEM-images of a CSB (a) and peripheral zone. In (E), grey is quartz and black is porosity. At the CSB periphery, grain indentation implies a pressure solution contact (b) and quartz-sealed intragranular fractures (authigenic quartz (c) appears in black). Note the very low fracture porosity (d) and preserved intergranular porosity (e) (Lower Permian, Piedra Larga fault zone). (G) Internal structure of a cataclasite featuring CSBs (a) and a well-developed S–C fabric in both CSBs and cataclastic host-sandstone (Tertiary, Pajonal fault zone; plain light microphotograph). (H) Detail of G (centre), showing a pressure solution clay and oxide-rich seam (black) marking the foliation (S). (I) Detail view in a CSB (same sample as that shown in (G) and (H)), showing a pressure solution contact (arrows) between quartz grain fragments (left) and a large quartz grain (right) (back-scattered SEM image). (J) Bedding-normal quartz-sealed vein (a) associated with stylolites (b) in low-porosity sandstone (Lower Devonian, Piedra Larga fault zone; plain light microphotograph).

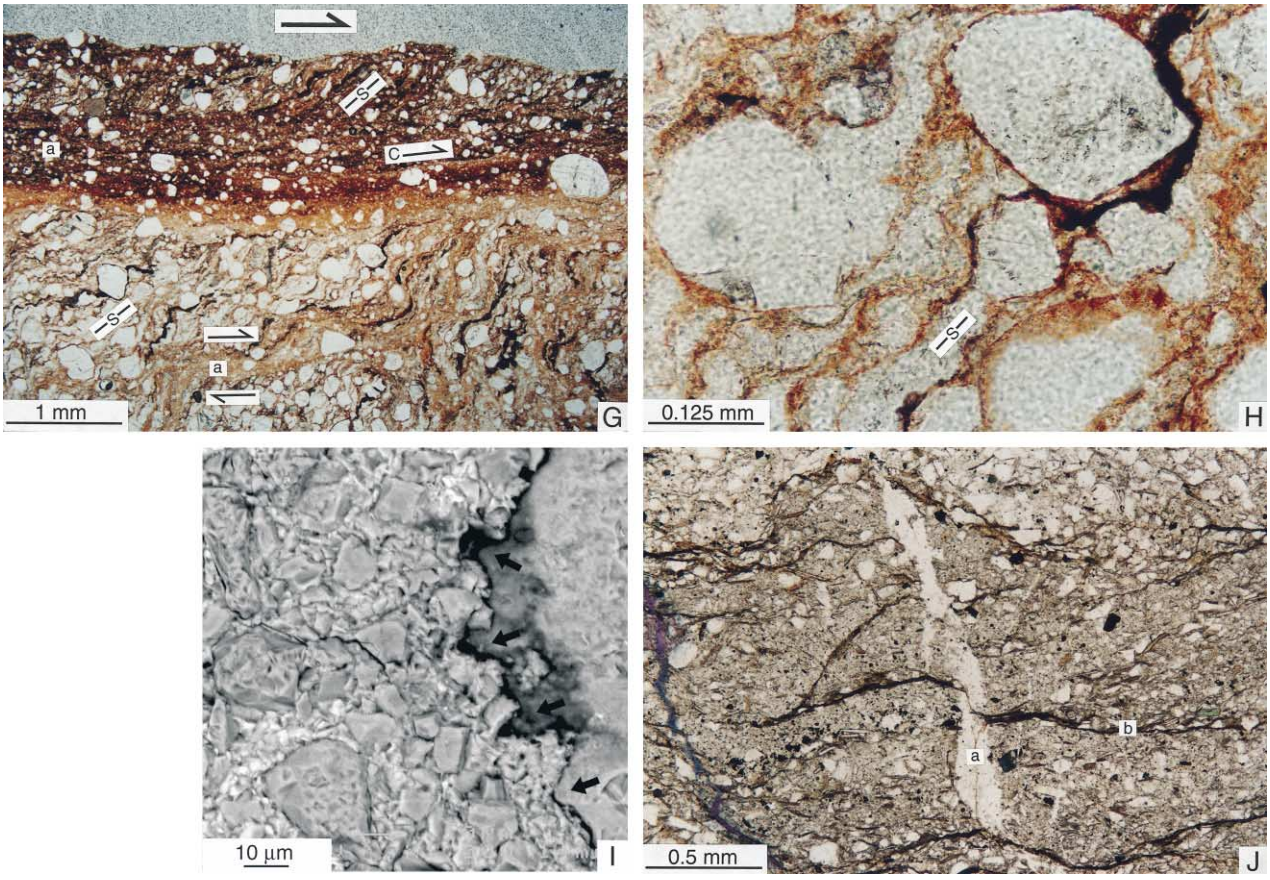

Fig. 9. (*continued*)

accelerates the transport of silica by reducing the length of the slowest diffusive path (Gratier et al., 1999).

- In the case of the CSBs, it is also possible that the strong grain-size reduction favoured free surface dissolution. Indeed, small fragments have a higher surface energy than the larger grains or fractures and this difference can promote diffusive transfer from small fragments to larger grain or fracture surfaces (Milliken, 1994; Dickinson and Milliken, 1995). Hence, this process may have contributed to the increase in the amount of dissolved silica close to fracture surfaces where precipitation occurred.
- Whatever the origin of quartz may be, fracturing is likely to accelerate quartz precipitation by increasing the surface/volume ratio close to the dissolution sites. These new surfaces are clean, which is also favourable for precipitation (Dickinson and Milliken, 1995; Fisher and Knipe, 1998; Fisher et al., 2000). This aspect may explain why, in many cases, quartz precipitated only in the fractures and not in the adjacent intergranular pores, where the occurrence of clay and oxide coating on the detrital grain surfaces probably inhibited the precipitation of overgrowths (Fig. 9C and E). Hence, fractures can form sinks for precipitation and contribute to prevent long-distance transport of the dissolved silica.

Although the considerations above suggest that most of the quartz cement was produced within the fault zone and transported over a short distance, it is possible that the fractures have also acted as sinks for silica dissolved by pressure solution at the periphery of the fault zone.

9.2. Factors controlling the occurrence of quartz sealing in fault zone microstructures

In the case of silica, the increase of temperature results in the increase of the dissolution/precipitation and, to a lesser degree, diffusion rates (Oelkers et al., 1996). The critical temperature range is 70–90°C because at lower temperatures the kinetics of quartz precipitation are very slow and, consequently, the silica transfer is very inefficient in geological processes. With higher temperatures, the kinetics of quartz precipitation are accelerated and, hence, silica transfer is possible and, in a system of diffusive transport, limited by the diffusion rate (Renard et al., 1997). We propose that this temperature-dependence of silica kinetics was the primary factor that controlled the occurrence of quartz-sealing in the SAZ fault zones. Other

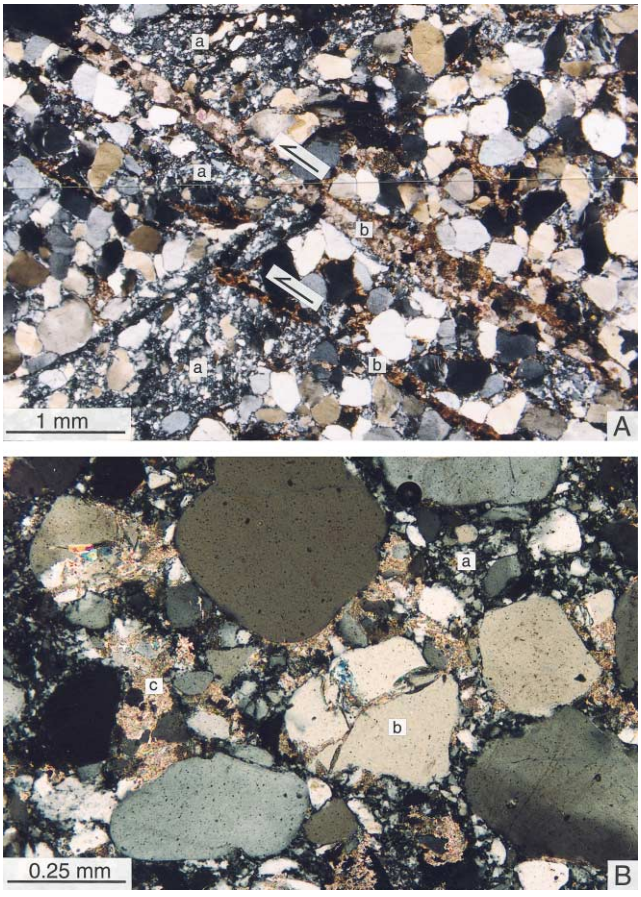

Fig. 10. Chronological relationship between quartz-sealed and later non-quartz-sealed microstructures. (A) Quartz-sealed cataclastic slip band (a) cross-cut and offset (arrows) by calcite-sealed fractures (Lower Permian, Piedra Larga fault zone). (B) Cataclasite featuring a first generation of quartz-sealed cataclasite (a) and a second generation of non-quartz-sealed grain fracturing (b) associated with calcite cement precipitation (c). Chronology is shown by the fact that calcite cement patches are secant on the older quartz-sealed cataclastic fabric (Tertiary, Pajonal fault zone).

factors such as grain size or the occurrence of clay may have contributed to accelerate or slow down the silica kinetics (e.g. Dewers and Ortoleva, 1990; Fisher and Knipe, 1998; Fisher et al., 2000; Renard et al., 2000). However, we observed microstructures with and without quartz sealing in sandstones of various grain sizes and clay contents, and thus these factors probably did not play a major role in the case studied here.

The consequence of this interpretation is that quartz-sealing distribution should have been a function of the depth at which the deformation was active. With the geothermal gradient of about 22°C/km and the average surface temperature of 15°C, which characterise the SAZ foredeep (Moretti et al., 1996; Husson and Moretti, 1999), the quartz-sealed microstructures would have developed below depths of about 2.5 km (70°C) to 3.4 km (90°C), whereas those without quartz-sealing would have developed at shallower depths. In this interpretation, the two types of deformation

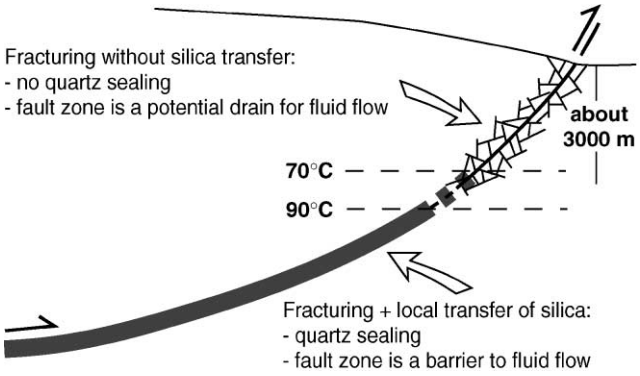

Fig. 11. Proposed model of temperature-dependent depth distribution of quartz sealing in a thrust fault zone.

were active simultaneously on a single fault at different depths (Fig. 11).

This interpretation corresponds with data from the North Sea, where recent works showed that normal fault zones buried to 3 km or more feature quartz-sealed cataclasites, whereas quartz sealing is lacking in shallower fault zones (Sverdrup and Bjørlykke, 1992; Fisher and Knipe, 1998; Fisher et al., 2000).

Chemical compaction related to sedimentary burial is also a process of diffusive silica transfer from pressure solution to precipitation sites (see above, Section 7) and temperature-dependence of quartz kinetics is also thought to be the main factor that controls its depth-distribution (Bjørlykke and Egeberg, 1993; Oelkers et al., 1996; Renard et al., 1999). The fact that, in the SAZ, chemical compaction was only observed in sandstones that reached maximal burial depths of at least around 3 km corresponds with this interpretation.

Although the discussion above implies that both chemical compaction related to sedimentary burial and fault-zone quartz sealing would develop below approximately the same depth, some differences can be expected because pressure solution and diffusive silica transport are time-dependent (Bjørkum et al., 1998; Renard et al., 1999). In the case of chemical compaction, the time-dependence results in an onset located at greater depth in recent sandstones with a high sedimentation rate. Hence, quartz cementation becomes significant at about 2.5 km depth in the Jurassic sandstones of the North Sea and at 3 and 4 km in the Miocene and Pliocene sandstones of the Gulf Coast, respectively (Bjørlykke and Egeberg, 1993). In the case of faults, one can expect that the rate of transfer is accelerated by stress and fracture formation in fault zones (see above) compared with chemical compaction at the same depth and, thus, the onset of fault zone quartz sealing may occur at shallower depth than that of chemical compaction. Another possibility is that some faults may have locally acted as drains for water in temperature disequilibrium with the host-rock, which would have also resulted in an onset of quartz sealing located higher than 3 km.

9.3. Observed distribution and chronology of fault zone quartz sealing in the SAZ

The inferred depth distribution of quartz-sealing in fault zones is coherent with three major facts (Fig. 3):

- Non-quartz-sealed microstructures are observed in all the studied fault zones, which were sampled at the surface or, in the case the Honduras well fault zone, at 2450 m depth where quartz sealing is also likely to be inhibited.
- Most of the observed quartz-sealed microstructures occur in Palaeozoic rocks that were buried at least 3 km deep when fault-deformation began, whereas the Tertiary sandstones most often show only non-quartz-sealed microstructures.
- Where quartz-sealed microstructures are present, they are always post-dated by the non-quartz-sealed microstructures. This can be explained by the fact that, for a given fault segment, the deformation conditions could also vary through time. In the foothills, due to anticline uplift and consecutive erosion contemporaneous with displacement along faults, the burial progressively decreased and, in critically buried fault zone segments, deformation could begin with quartz sealing and terminate without quartz sealing.

A few observations apparently do not fit with our model, but they may be explained as follows:

- The footwall fault core cataclasite in Tertiary sandstones at Pajonal is quartz-sealed. However, local lithological and structural features support the assumption that this cataclasite developed in a tectonic lens derived from the lower part of the Tertiary succession. This may be a case where fault zone quartz sealing developed at a depth shallower than for chemical compaction.
- Quartz-sealed microstructures are not observed in Palaeozoic rocks in some fault zones. At upper Camiri, Tunal and Aguarague, this may be due to pre-thrusting erosion (see above, Section 4) that would have resulted in shallow conditions during the whole deformation. At Rio Azero, Cuevo and Rio Pilcomayo, pre-thrust erosion is unlikely. However, in these cases, the density of fractures in fault zones is low and possible quartz-sealed fractures may have been missed due to the relatively low number of samples.

9.4. Implications on porosity, permeability and fluid flow

In the deep, quartz-sealed microstructures, quartz precipitation occurred quasi-simultaneously with fracture formation, resulting in microstructures with low porosity. In particular, the CSBs form virtually non-porous seams across host-sandstones that have often preserved original porosity (Fig. 9A–F). The CSBs forming a fault zone are usually connected, at least in the fault core, making the fault zone a band of rocks of lowered porosity with respect to the country rocks, i.e. a potential barrier to transversal fluid flow.

In the shallow, non-quartz-sealed microstructures, fracture porosity is preserved and carbonate cements are frequent (Figs. 6–8 and 10) and gypsum cements are occasionally present. Carbonate or gypsum precipitation was not intrinsic to deformation mechanisms as it was in the case of quartz precipitation. Since the SAZ sandstone bodies do not contain sedimentary carbonate or minerals likely to provide Ca ions (in particular, no Ca-feldspar grains), carbonate cements were necessarily imported by fluid flow from sources located outside sandstone bodies. The only important occurrence of gypsum veins, at Pajonal, occurs close to (i.e. up to a few tens of meters from) sedimentary gypsum deposits, which obviously constituted the sources for cement. This origin implies limited fluid flow for the transport of dissolved gypsum. It is interesting to note that the possible occurrence of abundant carbonate cement in CSBs (Fig. 8A) shows that they could be permeable to fluid flow, although previous work concluded that they have very low permeability (Antonellini and Aydin, 1994; Fowles and Burley, 1994). At the scale of fault zones, carbonate cement in microstructures and host-sandstone is often relatively abundant in fault zones, whereas it is absent or scarce in the adjacent country rocks (Fig. 3). This shows that the shallow, non-quartz-sealed fault zones were preferential pathways for longitudinal fluid flow, probably due to the high connectivity of fractures that increased permeability of the fault zones compared with the country rocks.

We note that our study excludes a significant strain dependence of fault zone sealing, since both quartz-sealed and unsealed microstructures occur in large-displacement fault zones (several tens of kilometres), as well as in small-displacement fault zones (<1 km). On the other hand, the stress regime may have played a role in fault zone permeability. Indeed, the existence of relief in the foothill anticlines is likely to result in an extensional stress regime at the surface (Sassi and Faure, 1997), which may favour fracture dilation, and therefore drainage in the shallow part of fault zones, whereas compressional stress at depth does not favour fault zone dilation.

The inferred distribution of fault zone quartz-sealing and its influence on fault permeability can explain the current role of faults in oil migration along the Andean front. In the foothills, the oil-seeps are often located at no more than a few hundred metres from the source rock (Middle–Upper Devonian) and hence the oil drainage distance is short and drainage is favoured by the occurrence of unsealed fractures and possible extensional stress. In contrast, reservoirs in the foredeep are buried to depths where faults are sealed by quartz, and hence lateral closure on fault can be efficient.

Discussing further the origin and conditions of carbonate-rich fluid and hydrocarbon migrations in fault zones is beyond the scope of this paper. The structural and chemical

characteristics of carbonate cementation in the SAZ fault zones and their implication for interpreting fluid drainage in the SAZ thrust system are presented separately (Labaume et al., 2000, 2001; Moretti et al., 2000).

10. Conclusion

In faulted sandstones, fracturing processes are largely controled by the initial porosity of the rocks, with intragranular fracturing (cataclasis) typical of porous sandstones and transgranular fractures typical of low-porosity sandstones. In the siliciclastic succession, about 10 km thick affected by the Neogene thrust faults of the Bolivian SAZ, the latter mechanism characterises deeply (>3 km) buried sandstones affected by pre-thrust chemical compaction, whereas the former mechanism characterises the porous sandstones of the upper part of the succession. However, the permeability of the SAZ fault rocks was not primarily controlled by these different mechanisms but by the occurrence or absence of quartz sealing. Quartz sealing may occur both in cataclasites and transgranular fractures and is related to local pressure solution and diffusive silica transport during deformation. Temperature is most probably the main factor that controls the activation of silica transfer and therefore we propose that the distribution of quartz sealing is a function of burial at the time of deformation. Consequently, fault zones must be sealed at depths exceeding about 3 km ($T > 70$–90°C), whereas shallower faults remain unsealed, which allowed most of them to be permeable to longitudinal carbonate-rich fluid flow. Due to foothill uplift during fault activity, erosion reduced burial and allowed non-quartz sealed fracturing to post-date quartz-sealed fracturing on critically buried fault segments. This distribution of quartz sealing and its implication on fault zone permeability are compatible with the fact that buried fault zones in the current foredeep seal hydrocarbon fields, whereas outcropping faults in the foothills localise numerous oil-seeps.

In conclusion, the major implication of this work is that the burial-related diagenetic conditions at the time of deformation are likely to be a first-order parameter in the evaluation of the sealing capacity of faults in sandstones. This parameter is independent of the type of fault (reverse or normal) and of the amount of fault offset.

Acknowledgements

We thank Yacimientos Petroliferos Fiscales Bolivianos for access to data and support during field work. We are especially grateful to our Bolivian colleagues, J. Oller, G. Montemuro, E. Aguillera and E. Mendez. We thank Y. Géraud for Hg-porosimetry measurements at Strasbourg University, B. Lanson for kaolin analyses at Grenoble University, E. Rosenberg and P. Guéroult for SEM imaging at IFP, and Ph. Blanc for CL–SEM imaging at Paris VI University. J.P. Gratier, A.M. Boullier and F. Renard are greatly acknowledged for fruitful discussions and criticism during this study, as well as K. Bjørlykke and J.P. Evans for their constructive reviews of the original manuscript. The work was funded by Elf, Maxus and Pluspetrol, and partially by Repsol, Mobil and Exxon.

References

Antonellini, M., Aydin, A., 1994. Effect of faulting on fluid flow in porous sandstones: petrophysical properties. American Association of Petroleum Geologists Bulletin 78, 355–377.

Antonellini, M., Aydin, A., Pollard, D., 1994. Microstructure of deformation bands in porous sandstones at Arches National Park. Journal of Structural Geology 16, 941–959.

Aydin, A., Johnson, A.M., 1983. Analysis of faulting in porous sandstones. Journal of structural Geology 5, 19–31.

Baby, P., Guillier, B., Oller, J., Herail, G., Montemurro, G., Zubieta, D., Specht, M. 1993. Structural synthesis of the Bolivian Subandean zone. International Symposium on Andean Geodynamics. Abstracts of Proceeding, ORSTOM (Série Colloques et Séminaires), pp. 159–162.

Berthé, D., Choukroune, P., Jegouzo, P., 1979. Orthogneiss mylonite and non coaxial deformation of granites: the example of the South-Armorican shear zone. Journal of Structural Geology 1, 31–42.

Bjørkum, A., Oelkers, E.H., Nadeau, P.H., Walderhaug, O., Murphy, W.M., 1998. Porosity prediction in quartzose sandstones as a function of time, temperature, depth, stylolite frequency, and hydrocarbon saturation. American Association of Petroleum Geologists Bulletin 82, 637–648.

Bjørlykke, K., 1994. Fluid-flow processes and diagenesis in sedimentary basins. In: Parnell, J. (Ed.). Geofluids: origin, migration and evolution of fluids in sedimentary basins. Geological Society Special Publication 78, pp. 127–140.

Bjørlykke, K., Egeberg, P.K., 1993. Quartz cementation in sedimentary basins. American Association of Petroleum Geologists Bulletin 77, 1538–1548.

Caine, J.S., Evans, J.P., Forster, C.B., 1996. Fault zone architecture and permeability structure. Geology 24, 1025–1028.

Chester, F.M., Logan, J.M., 1986. Implications for mechanical properties of brittle faults from observations of the Punchbowl fault zone, California. Pure and Applied Geophysics 124, 79–106.

Chester, F.M., Friedman, M., Logan, J.M., 1985. Foliated cataclasites. Tectonophysics 111, 139–146.

Colletta, B., Letouzey, J., Soares, J., Specht, M. 1999. Detachment versus fault-propagation folding: insights from the Sub-Andean Ranges of southern Bolivia. Thrust Tectonics Conference. Abstracts of Proceedings, Royal Holloway, University of London, pp. 106–109.

Dewers, T., Ortoleva, P., 1990. A coupled reaction/transport/mechanical model for intergranular pressure solution stylolites, and differential compaction and cementation in clean sandstones. Geochimica et Cosmochimica Acta 54, 1609–1625.

Dickinson, W.W., Milliken, K.L., 1995. The diagenetic role of brittle deformation in compaction and pressure solution, Etjo Sandstone, Namibia. Journal of Geology 103, 339–347.

Ehrenberg, S.N., Aagaard, P., Wilson, M.J., Fraser, A.R., Duthie, D.M.L., 1994. Depth-dependent transformation of kaolinite to dickite in sandstones of the Norwegian continental shelf. Clay Minerals 28, 325–352.

Evans, J.P., 1988. Deformation mechanisms in granitic rocks at shallow crustal levels. Journal of Structural Geology 10, 437–443.

Fisher, Q.J., Knipe, R.J., 1998. Fault sealing processes in siliciclastic sediments. In: Jones, G., Fisher, Q.J., Knipe, R.J. (Eds.). Faulting,

Fault Sealing and Fluid Flow in Hydrocarbon Reservoirs. Geological Society Special Publication 147, pp. 117–134 .

Fisher, Q.J., Knipe, R.J., Worden, R.H., 2000. Microstructures of deformed and non-deformed sandstones from the North Sea: implications for the origin of quartz cement in sandstones. In: Worden, R., Morad, S. (Eds.). Quartz Cementation in Sandstones. International Association of Sedimentologists Special Publication 29, pp. 129–146.

Fowles, J., Burley, S., 1994. Textural and permeability characteristics of faulted, high-porosity sandstones. Marine and Petroleum Geology 11, 608–623.

Gratier, J.P., Renard, F., Labaume, P., 1999. How pressure solution and fracturing processes interact in the upper crust to make it behave as both brittle and viscous. Journal of Structural Geology 21, 1189–1197.

Green II, H.W., 1984. "Pressure solution" creep: some causes and mechanisms. Journal of Geophysical Research 89, 4313–4318.

Gubbels, T.L., Isacks, B.L., Farrar, E., 1993. High-level surfaces, plateau uplift, and foreland development, Bolivian central Andes. Geology 21, 695–698.

Houseknecht, D.W., 1988. Intergranular pressure solution in four quartzose sandstones. Journal of Sedimentary Petrology 58, 228–246.

Husson, L., Moretti, I. 1999. Thermal controls in compressive zones. An example from the Bolivian Sub-Andean Zone. Fourth International Symposium on Andean Geodynamics. Abstracts of Proceedings, University of Göttingen (Germany), pp. 347–351.

Kley, J., Gangui, A.H., Krüger, D., 1996. Basement-involved blind thrusting in the eastern Cordillera Oriental, southern Bolivia: evidence from cross-sectional balancing, gravimetric and magnetotelluric data. Tectonophysics 259, 171–184.

Knipe, R.J., 1997. Juxtaposition and seal diagrams to help analyse fault seals in hydrocarbon reservoirs. American Association of Petroleum Geologists Bulletin 81, 187–195.

Labaume, P., Moretti, I. 1997. Thrust-faulting, fluid flow and hydrocarbon migration in the Andean foothills. In: Hendry, J., Carey, P., Parnell, J., Ruffell, A., Worden, R. (Eds.), Geofluids II Conference. Abstracts of Proceedings, The Queen's University of Belfast, pp. 111–114.

Labaume, P., Sheppard, S., Moretti, I., 2000. Structure and hydraulic behaviour of cataclastic thrust fault zones in sandstones, Sub-Andean Zone, Bolivia. Journal of Geochemical Exploration 69-70, 487–492.

Labaume, P., Sheppard, S., Moretti, I., 2001. Fluid flow in cataclastic thrust fault zones in sandstones, Sub-Andean Zone, Bolivia. Tectonophysics, in press.

Lin, A., 1999. S–C cataclasite in granitic rocks. Tectonophysics 304, 257–273.

Lister, G.S., Snoke, A.W., 1984. S–C mylonites. Journal of Structural Geology 6, 617–638.

Logan, J.M., Dengo, C.A., Higgs, N.G., Wang, Z.Z., 1992. Fabrics of experimental shear zones: their development and relationships to mechanical behavior. In: Evans, B., Wong, T.F. (Eds.). Fault Mechanics and Transport Properties of Rocks. Academic Press, New York, NY, pp. 34–67.

Mair, K., Main, I., Elphick, S., 2000. Sequential growth of deformation bands in the laboratory. Journal of Structural Geology 22, 25–42.

Milliken, K.L., 1994. The widespread occurrence of healed microfractures in siliciclastic rocks: evidence from scanned cathodoluminescence images. In: Nelson, Laubach (Eds.). Rock Mechanics. Balkema, Rotterdam, pp. 825–832.

Mitra, G., 1984. Brittle to ductile transition due to large strains along the White Rock thrust, Wind River mountains, Wyoming. Journal of Structural Geology 6, 51–61.

Moretti, I., 1998. The role of faults in hydrocarbon migration. Petroleum Geosciences 4, 81–94.

Moretti, I., Baby, P., Mendez, E., Zubieta, D., 1996. Hydrocarbon generation in relation to thrusting in the Sub Andean Zone from 18 to 22°S, Bolivia. Petroleum Geosciences 2, 17–28.

Moretti, I., Labaume, P., Sheppard, S., Boulègue, J., 2000. Compartmentalisation of fluid flow by thrust faults, Sub-Andean Zone, Bolivia. Journal of Geochemical Exploration 69-70, 493–497.

Oelkers, E.H., Bjørkum, P.A., Murphy, W.M., 1996. A petrographic and computational investigation of quartz cementation and porosity reduction in North Sea sandstones. American Journal of Science 296, 420–452.

Pedersen, T., Bjørlykke, K., 1994. Fluid flow in sedimentary basins: a model of water flow in a vertical fracture. Basin Research 6, 1–16.

Renard, F., Ortoleva, P., Gratier, J.P., 1997. Pressure solution in sandstones: influence of clays and dependence on temperature and stress. Tectonophysics 280, 257–266.

Renard, F., Park, A., Ortoleva, P., Gratier, J.P., 1999. An integrated model for transitional pressure solution in sandstones. Tectonophysics 312, 97–115.

Renard, F., Brosse, F., Gratier, J.P., 2000. The different processes involved in the mechanism of pressure solution in quartz-rich rocks and their interactions. In: Worden, R., Morad, S. (Eds.), Quartz Cementation in Sandstones. International Association of Sedimentologists Special Publication 29, pp. 67–78.

Rutter, E.H., 1983. Pressure solution in nature, theory and experiments. Journal of the Geological Society 140, 725–740.

Sassi, W., Faure, J.L., 1997. Role of faults and layer interfaces on the spatial variation of stress regimes in basins: inferences from numerical modeling. Tectonophysics 266, 101–119.

Schneider, F., Devoitine, H., Faille, I., Flauraut, E., Willien, F., Wolf, S., 1999. A new 2D basin modeling tool for HC potential evaluation in faulted area. Applications to the Congo offshore and to the Bolivian sub-Andean zone. Hedberg Conference on Multi-dimensional basin modeling. Abstracts of Proceedings, American Association of Petroleum Geologists.

Schulz, S.E., Evans, J.P., 1998. Spatial variability in microscopic deformation and composition of Punchbowl fault, southern California: implication for mechanisms, fluid-rock interaction, and fault morphology. Tectonophysics 295, 223–244.

Sempere, T., 1995. Phanerozoic evolution of Bolivia and adjacent regions. In: Tankard, A.J., Suarez, S., Welsink, H.J. (Eds.). Petroleum Basins of South America. American Association of Petroleum Geologists Memoir 62, pp. 207–230.

Sverdrup, E., Bjørlykke, K., 1992. Small faults in sandstones from Spitsbergen and Haltenbanken. A study of diagenetic and deformational structures and their relation to fluid flow. In: Larsen, R.M., Brekke, H., Larsen, B.T., Telleraas, E. (Eds.). Structural and Tectonic Modelling and its Applications to Petroleum Geology. Norwegian Petroleum Society Special Publication 1, pp. 507–517.

Yielding, G., Freeman, B., Needham, D.T., 1997. Quantitative fault seal prediction. American Association of Petroleum Geologists Bulletin 81, 897–917.